JVI Journals.ASM.org

Measles Virus Transmission from Dendritic Cells to T Cells: Formation of Synapse-Like Interfaces Concentrating Viral and Cellular Components

Susanne Koethe, Elita Avota, and Sibylle Schneider-Schaulies

Institute for Virology and Immunobiology, University of Wuerzburg, Wuerzburg, Germany

Transmission of measles virus (MV) to T cells by its early CD150$^+$ target cells is considered to be crucial for viral dissemination within the hematopoietic compartment. Using cocultures involving monocyte-derived dendritic cells (DCs) and T cells, we now show that T cells acquire MV most efficiently from *cis*-infected DCs rather than DCs having trapped MV (*trans*-infection). Transmission involves interactions of the viral glycoprotein H with its receptor CD150 and is therefore more efficient to preactivated T cells. In addition to rare association with actin-rich filopodial structures, the formation of contact interfaces consistent with that of virological synapses (VS) was observed where viral proteins accumulated and CD150 was redistributed in an actin-dependent manner. In addition to these molecules, activated LFA-1, DC-SIGN, CD81, and phosphorylated ezrin-radixin-moesin proteins, which also mark the HIV VS, redistributed toward the MV VS. Most interestingly, moesin and substance P receptor, both implicated earlier in assisting MV entry or cell-to-cell transmission, also partitioned to the transmission structure. Altogether, the MV VS shares important similarities to the HIV VS in concentrating cellular components potentially regulating actin dynamics, conjugate stability, and membrane fusion as required for efficient entry of MV into target T cells.

Measles virus (MV), which remains one of the major causes of vaccine-preventable infant death worldwide, is highly contagious and infects via the respiratory tract. Professional antigen-presenting cells, such as bronchial macrophages and/or dendritic cells (DCs), penetrating through the deep lung epithelium, rather than epithelial cells, are early targets of infection (5, 13, 29). In line with earlier suggestions, these cells are believed to serve as Trojan horses mediating MV transport to secondary lymphatics, where they induce MV-specific immunity, yet where generalized immunosuppression by this virus also occurs (15, 35, 37, 41). For the latter, inadequate expression levels of major histocompatibility complex and costimulatory molecules, inhibitory signals conveyed to scanning T cells by MV proteins displayed at the DC membrane, and immune synapse instability potentially related to the release of repulsive mediators have been suggested to contribute to impaired T cell responses upon *in vitro* restimulation (17, 26, 42, 46). Alternatively, transmission of infectious MV to T cells, followed by syncytium formation *in vitro* (8, 16), as well as infection-mediated loss of especially activated and/or memory cells *in vivo*, has been linked to both MV induced lymphopenia and immunosuppression (31, 36). In addition to this, MV transmission to lymphocytes, including T cells in lymphoid tissues, is essential for viral dissemination and spread (1, 5, 27, 47).

Viral DC-T cell transmission, extensively studied for HIV, either relies on DC infection (*cis*-infection) or mere viral capture (mainly by C-type lectin receptors), followed by viral transfer to target T cells (*trans*-infection) (12). In common with HIV, MV is captured by C-type lectin receptors such as Langerin or DC-SIGN on Langerhans cells (LCs) or DCs (7). While LCs barely support *cis*-infection by MV, which is instead sorted to Birbeck granules (48), MV enters into and replicates in myeloid DCs, and this is dependent on the expression of CD150, the MV entry receptor on hematopoietic cells *in vitro* and *in vivo* (4–8, 50). Because DC-SIGN$^+$ cells with DC morphology did not detectably display CD150 on their surfaces in healthy deep respiratory tract tissues, these cells were considered as primarily capturing MV via DC-SIGN and, thus, MV transmission to T cells would mainly occur by *trans*-infection (8). However, DC-SIGN ligation was recently found to cause vertical transport of CD150 to the plasma membrane from an intracellular storage compartment (2), thus supporting extensive evidence for MV *cis*-infection of these cells obtained *in vitro* and *in vivo* (5, 13).

For HIV, cell-associated transmission to T cells was found to be up to 100-fold more efficient than cell-free transmission and relies on the formation of spatially organized interfaces referred to as virological synapses (VS), which require lateral sorting of HIV receptors, as well as the recruitment of tetraspanins, especially CD81, moesin, and integrins (3, 18, 32). Moreover, actin rearrangements that accompany HIV transfer can also be mediated by actin-containing processes (filopodial bridges or nanotubes) (for a recent review, see references 28 and 45). Although MV transmission from DCs to T cells has been demonstrated in cocultures and although both the importance of CD150 on T cells in this process and the formation of extensions has been revealed (8, 16), the relative efficiency of this MV transmission has not been directly assessed, nor has VS formation or the components thereof been analyzed. Using an autologous coculture system, we now show that MV transmission to T cells most efficiently occurs from *cis*-infected DCs, and this involves the formation of polyconjugates and an organized VS. There, the viral proteins concentrate on the DC interface, while CD150 is redistributed in an actin-dependent

Received 22 February 2012 Accepted 25 June 2012
Published ahead of print 3 July 2012
Address correspondence to Sibylle Schneider-Schaulies, s-s-s@vim.uni-wuerzburg.de.

doi:10.1128/JVI.00458-12

process toward the contact site. Also in common with the HIV VS, moesin, in addition to CD81, is recruited to this site, as is the substance P receptor (SPR) HNK-1, both of which have previously been implicated in the enhancement of MV infection of target cells (10, 20, 38), indicating that the MV VS concentrates both viral proteins and surface receptors involved in interface stabilization and MV entry.

MATERIALS AND METHODS

Ethics statement. Primary human cells were obtained from the Department of Transfusion Medicine, University of Wuerzburg, and analyzed anonymously. All experiments involving human material were conducted according to the principles of the Declaration of Helsinki and ethically approved by the Ethical Committee of the Medical Faculty of the University of Wuerzburg.

Cells, stimulation, and viruses. Monocytes and T cells were enriched from peripheral blood by Ficoll gradient centrifugation, followed by plastic adherence, and by using nylon wool columns, respectively. Both cell types were maintained in RPMI 1640 containing 10% fetal calf serum (FCS), which was supplemented by human granulocyte-macrophage colony-stimulating factor (GM-CSF; 500 U/ml; Berlex, Germany)–interleukin-4 (IL-4; 250 U/ml; Miltenyi Biotec, Germany) for 3 to 6 days for the generation of immature DCs. When indicated, T cells were activated by phorbol myristate acetate (PMA; 40 ng/ml)–ionomycin (0.5 μM; Sigma-Aldrich) or αCD3 (UCHTI; 1 μg/ml)-αCD28 (CD28.2; 1 μg/ml) (both from Becton Dickinson) for 20 min on ice, followed by cross-linking by plate-bound goat anti-mouse IgG (5 μg/ml; Dianova) for 48 h, washing, and addition to DCs.

MV wild-type strain (WTF; genotype C2) grown on BJAB cells and a recombinant MV (IC323-eGFP [kindly provided by Y. Yanagi]) grown on Vero cells stably expressing CD150 (both kept in RPMI 1640–10% FCS) were titrated on marmoset lymphoblastoid B95a cells (in RPMI 1640–5% FCS). Mock preparations were prepared from frozen-thawed BJAB cells, followed by centrifugation. DCs were analyzed 24 h after infection using a multiplicity of infection of 1 (WTF-DCs or IC323-eGFP-DCs, respectively), followed by the addition of a fusion inhibitory peptide Z-D-Phe-L-Phe-Gly-OH to prevent spread and syncytium formation (Bachem; 200 μM in dimethyl sulfoxide; also added to mock cultures). Infection levels ranged between 20 and 40%, as determined by flow cytometry (see below).

Antibodies. MV proteins were detected using monoclonal antibodies (MAbs) directed against N (F227) or H (K83, NC32, and L77) proteins or MV P-specific rabbit serum (all generated in our laboratory). IgG1 CD3- and CD25-specific MAbs (directly conjugated to phycoerythrin [both obtained from Becton Dickinson]), CD150-specific MAbs IPO3 (Cayman Chemicals) and 5C6 (generated in our laboratory), or isotype control IgG1 (I1; directed against the vesicular stomatitis virus G protein) were used for flow cytometry. For immunofluorescence analyses, we used the following MAbs: hemagglutinin (HA) tag-specific F-7 (Santa Cruz Biotechnology), ICAM-1-specific MAb (R&D Systems), LFA-1 α-chain CD11a-specific MAb NKI-L16 (which recognizes a Ca^{2+}-dependent epitope and was kindly provided by C. Figdor), CD81-specific MAb Z81.1 and moesin-specific MAb 38/87 (both kindly provided by J. Schneider-Schaulies), pERM-specific MAb 41A3 (Cell Signaling), and DC-SIGN-specific MAb H200 (Santa Cruz Biotechnology). We also used a polyclonal rabbit antiserum directed against the cytoplasmic tail of substance P receptor (generated in our laboratory; the specificity was tested on CHO cells stably expressing substance P receptor [SPR; kindly provided by J. Krause]). Primary antibodies were either directly labeled (Zenon Alexa Fluor 594 mouse IgG1 labeling kit [Invitrogen]) or detected using goat $F(ab')_2$ fragment anti-mouse IgG(H+L)-A594, chicken anti-rabbit IgG(H+L)-A594, and goat anti-mouse IgG(H+L)-A647 (all from Invitrogen) as secondary antibodies. DRAQ5 (Invitrogen) was used for nuclear stains. F-actin was detected using phalloidin-A488, and cell labeling was performed using wheat germ agglutinin (WGA) conjugated to A488 or octadecyl rhodamine B (R18) (all from Invitrogen).

Transmission assays. DCs (5×10^4) used 24 h after infection (*cis*-MV-DCs) or after 1 to 2 h after loading with MV and subsequent washing (*trans*-MV-DCs) were cocultured with autologous T cells (2×10^5) at a ratio of 1:4 for 2 h (unless stated otherwise) in RPMI 1640–10% FCS supplemented with GM-CSF and IL-4, which was also used for subsequent washing and maintenance, with fusion inhibitory peptide (FIP) added to prevent further transmission (8). For blocking experiments, cells were exposed to isotype control (I1), CD150 (5C6), and MV H (clones L77 and NC32) antibodies, all at 100 μg/ml, or to CD81 antibody (at 50 μg/ml) for 1 h at 37°C prior to onset of the coculture.

Transmission efficiencies were determined after 3 days of coculture by detection of live green fluorescent protein-positive (GFP^+) cells or, when unlabeled MV (WTF) was used, by detection of fixed MV N expressing $CD3^+$ cells by flow cytometry. For the detection of $CD3^+$ GFP^+ cells, T cell populations were first gated based on forward scatter-side scatter (FSC/SSC) and, subsequently, on the $CD3^+$ population within which the frequency of GFP^+ cells was determined. Exclusion of DCs by FSC/SSC gating was necessary because they reveal a high GFP autofluorescence, as described earlier (8). Experiments (routinely performed in duplicates) were repeated three times using independent donors.

Conjugate analyses. DCs at 5×10^4 (MV-infected DCs or WGA-labeled mock-infected DCs [Mock-DCs]) were seeded per poly-L-lysine-coated chamber slide for 30 min at 37°C prior to the addition of autologous T cells (2×10^5) for 1 h in RPMI 1640–10% FCS with GM-CSF and IL-4. When indicated, T cells were transfected with pCG-CD150-HA using an Amaxa human T cell nucleofector kit (Lonza) and used 24 h later for conjugate formation. Conjugates were fixed in phosphate-buffered saline (PBS) containing 4% paraformaldehyde prior to antibody staining (each diluted in PBS–1% bovine serum albumin), fluorochrome G mounted (Southern Biotech), and examined using confocal laser scanning microscopy (LSM510 Meta; software version 3.0; Axiovert 200 microscope; objective, ×100; NA, 1.4 Plan Apochromat). At least 20 conjugates/per staining experiment were analyzed; the scale bars in all image panels represent 10 μm. For quantification, the frequency of conjugates revealing a pronounced accumulation of the respective compound at extended VS interfaces was determined. For this, the three fluorescence color images were split (to obtain each color singly) and transformed into black-and-white representations. Within these, the cells of interest were analyzed for total pixel intensities (yielding the total amount of the given protein per cell, which was set to 100%) and pixel intensities in gated VS areas (quantified then as the percent VS redistribution compared to the total pixel intensities) using AIDA software. VS redistribution was assigned if the intensities observed differed significantly from those seen in surface areas other than the VS (or the interface formed with Mock-DCs, respectively). For the immunofluorescence analysis, statistical significance (indicated in the figures by asterisks as defined in the legends) was determined using GraphPad Prism software and the Student *t* test for the transmission quantitative experiments by one-way analysis of variance, followed by Bonferroni post-testing.

RESULTS

Efficient MV transmission to T cells relies on DC *cis*-infection. To comparatively address the efficiency of cell-free versus cell-associated infection of T cells, the cells were left unstimulated or were activated by PMA-ionomycin (P/I) or αCD3/CD28 antibodies 24 h prior to exposure to MV alone (MV) or autologous immature DCs (iDCs) infected with a recombinant MV expressing eGFP as an extra reading frame (IC323-eGFP) 1 day earlier (referred to as *cis*-MV-DCs), or DCs were loaded with MV 2 h prior to coculture (*trans*-MV-DCs) (Fig. 1). Transmission/infection was limited to a time window of 2 h, after which FIP was added to prevent further viral transfer to T cells. Within this time frame, the

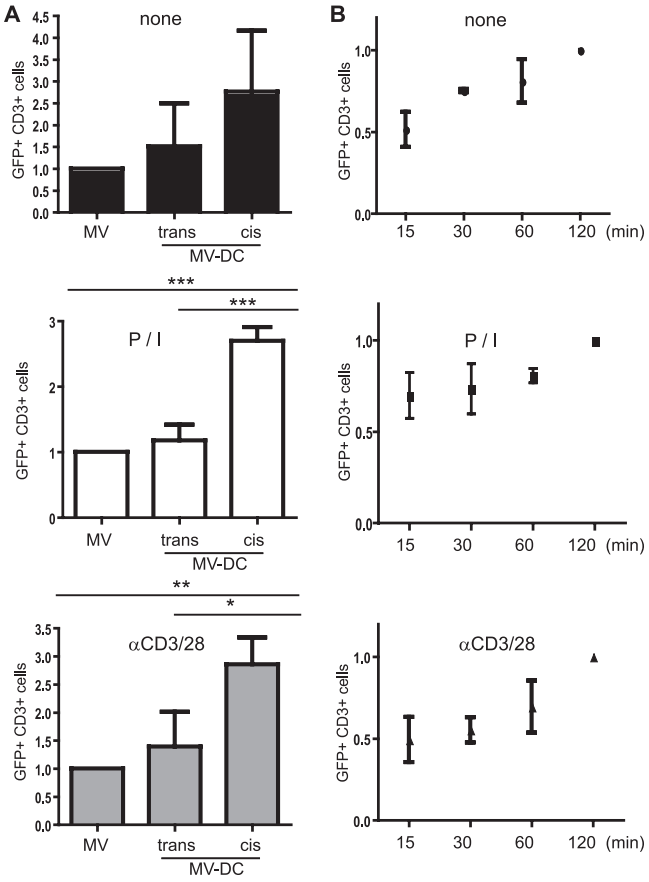

FIG 1 MV *cis*-infection of T cells is most efficient and time dependent. *trans*- or *cis*-MV transmission involved IC323-eGFP-DCs cocultured with autologous T cells (ratio, 1:4) for 2 h (A) or IC323-eGFP-*cis*-DCs for the time intervals indicated (B). FIP was then added to prevent further transmission. The frequencies of $GFP^+/CD3^+$ cells were determined after 3 days by flow cytometry and compared to those seen in T cell cultures having received MV in the absence of DCs (MV) (A) or to the frequencies seen 2 h after transmission (B). The means of three independent experiments (each performed in duplicates) are indicated by error bars representing the standard deviations. The frequencies of $GFP^+/CD3^+$ cells in cell-associated transmission assays were normalized to the respective cell-free virus acquisition. *, $P < 0.05$; **, $P < 0.01$; ***, $P < 0.001$.

production of MV from loaded DCs can be excluded, since only receptor-trapped MV can be transmitted by these cells. At 3 days after MV transfer to T cells, the frequencies of infected (GFP^+) $CD3^+$ cells in all cultures were analyzed by flow cytometry, and these values did not exceed 0.8% in cocultures involving mock-infected DCs or T cells exposed to mock preparations (used for this and all following experiments [data not shown]). Irrespective of the T cell activation status, the acquisition of MV was, on average, almost twice as efficient from *cis*-MV-DCs (compared to that seen with *trans*-infection or cell-free infection, which did not significantly differ from each other) (Fig. 1A). Thus, frequencies of GFP^+ cells acquired on cell free and *trans*-infection did not exceed 18%, while, on average, 52 and 36% of the $CD3^+$ cells expressed GFP when P/I-activated and αCD3/CD28-activated T cells had acquired MV via *cis*-infected DCs. The kinetics of MV transmission from *cis*-infected DCs to unstimulated or preactivated T cells did not markedly differ, as revealed in experiments where the time window for transmission was narrowed to 15, 30, or 60 min rather than 120 min (Fig. 1B). Thus, transmission was most efficient from *cis*-MV-DCs to preactivated T cells, and therefore this system was used for further analyses.

MV transmission involves the MV glycoproteins and CD150 on the target T cell. Because receptor interaction might play an essential role in enhancement of T cells infection by *cis*-MV-DCs, we confirmed that both P/I and αCD3/CD28 stimulation promoted the surface display of CD150 (and CD25 included as activation control) on T cells (Fig. 2A). In line with the importance of MV receptor interaction in this process, *cis*-MV-DC-mediated transmission was substantially affected by the blocking of CD150 on T cells (Fig. 2B) or the blocking of MV-DCs with HA-specific, but not CD150-specific antibodies (Fig. 2C and data not shown for CD150). Altogether, these observations identify *cis*-infected DCs as efficiently mediating MV transmission to T cells, and this process is sensitive to antibodies blocking the interaction between the entry receptor CD150 and its ligand, the MV H protein.

MV-DC/T cell interfaces concentrate CD150 and MV proteins, consistent with VS formation. To gain insight into the spatial organization of MV transmission sites, we first determined the frequencies of T cells conjugating to autologous MV-infected versus Mock-DCs, which were visualized by labeling with A488-conjugated WGA. Unstimulated T cells conjugated to Mock-DCs and MV-DCs with similar efficiencies, whereas preactivated T cells tended to be recruited into polyconjugates with GFP^+ MV-DCs, thereby increasing the potential frequency of transmission sites (Fig. 3A). GFP^- DCs in these cultures did not differ with regard to T cell conjugation from Mock-DCs (data not shown). Consistent with the formation of the VS, the accumulation of both F-actin and MV H proteins was detected at interfaces formed between preactivated T cells and MV-DCs (Fig. 3B, left panels with actin accumulation shown by intensity representation). MV H protein was also associated with F-actin-enriched extensions in these cultures, confirming earlier observations that transmission may also involve filopodial bridges (Fig. 3B, right panels). These were, however, rarely seen, and thus we concentrated on the VS as a major transmission site further on.

To describe the accumulation of compounds in the VS, we set out to determine the frequency of conjugates (with each at least 20 conjugates analyzed per condition), where a substantial concentration of the protein of interest at extended interfaces compared to juxtaposed membrane areas was revealed by false color analysis in intensity representations. Substantial VS redistribution of CD150 was seen in conjugates involving MV-infected DCs but not WGA-labeled mock-exposed DCs (Fig. 4A). As noted earlier (Fig. 3A), DCs conjugating several T cells were frequently observed. CD150 expression in iDCs is low (2, 8), did not markedly increase by 24 h postinfection (not shown), and thus might not essentially contribute to the CD150 VS concentration. To verify that the CD150 redistribution efficiently occurs at the acceptor cell surface (where it proved to be important for transmission [Fig. 2C]), T cells transfected to express HA-tagged CD150 were used for conjugate analyses. There, the tagged CD150 almost completely localized at the contact sites (Fig. 4B), and its redistribution on T cells proved to be actin dependent, because it was efficiently impaired on pretreatment of transfected T cells (left unstimulated or P/I activated) by latrunculin B but not nocodazole (Fig. 4C). As observed for its entry receptor on T cells, MV H protein displayed in patches on the surfaces of MV-DCs in the absence of T cells (data not shown) was efficiently recruited to the VS, thereby supporting

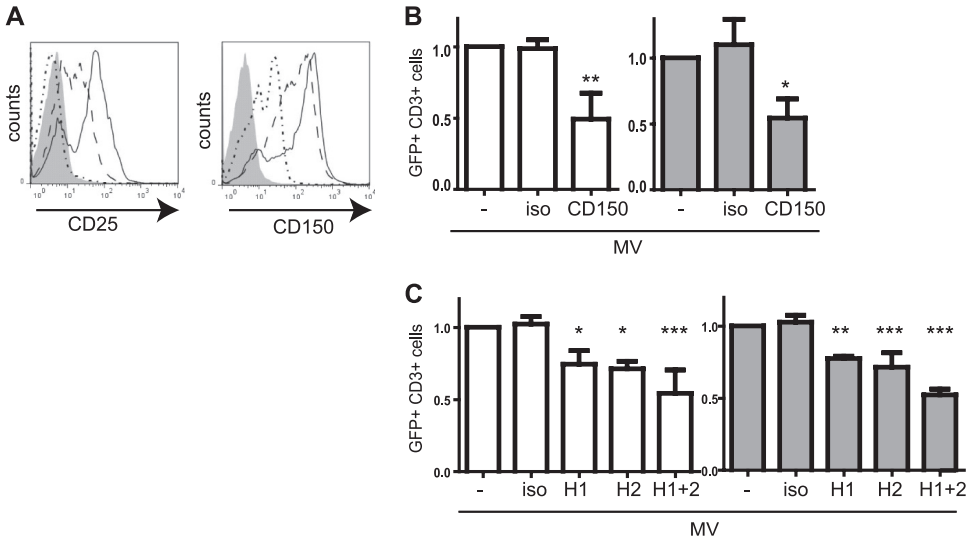

FIG 2 MV transmission depends on CD150 and H protein. (A) CD25 and CD150 expression levels were determined in T cells either left unstimulated (dotted line), stimulated with P/I (hatched line), or stimulated with αCD3/CD28 (solid line) by flow cytometry (gray profile, isotype control). (B and C). The frequencies of $GFP^+/CD3^+$ cells were determined 3 days after coculture of IC323-eGFP-DC with autologous T cells (P/I activated, white bars; αCD3/CD28 activated, gray bars), wherein T cells were exposed to CD150-specific antibodies (B) or DCs were exposed to MV H-specific antibodies (H1, NC32; H2, L77) (C) or the respective isotype antibodies (iso) for 1 h prior to transmission. The results were normalized to the untreated controls. The means of three independent experiments (each performed in duplicates) are indicated by error bars representing the standard deviations. Significance levels were determined for differences from untreated cells (set to 1) (*, $P < 0.05$; **, $P < 0.01$; ***, $P < 0.001$).

its function as a transmission compartment (Fig. 4D). In support of this hypothesis, MV P protein detected as a representative RNP component also efficiently accumulated at these sites (Fig. 4D). In contrast to CD150 T cells, the role of actin in VS redistribution of MV proteins in DCs (and that of all other proteins analyzed thereafter) in conjugates could not be analyzed because the pretreatment of DCs with latrunculin B (LatB) or nocodazole strongly affected the substrate adhesion of conjugates (data not shown). Thus, transmission of MV from *cis*-MV-DCs to T cells involves concentration of viral proteins and CD150 in a VS.

ICAM-1, LFA-1, CD81, pERM, and substance P receptor are components of the MV VS. Because ICAM-1, activated LFA-1, and the tetraspanin CD81 have already been shown to be constituents of the HIV infectious synapse, we analyzed whether, in addition to F-actin, they would localize to the synapse formed between MV-DCs and activated T cells. Although there was an obvious tendency for VS accumulation of F-actin (Fig. 3B), its VS redistribution did not reach statistical significance, whereas that of ICAM-1 and LFA-1 to this site was clearly detectable (Fig. 5A, upper panels and right diagrams). In addition, CD81 and DC-SIGN also concentrated at the VS (Fig. 5A, bottom panels and right diagrams), indicating that, in common with the HIV VS, CD81 not only marks the MV VS but MV transmission was also partially blocked when DCs were pretreated with anti-CD81 antibodies prior to transmission (Fig. 5B). Again, in common with the HIV VS, phosphorylated ezrin-radixin-moesin (ERM) family members clearly redistributed to the MV VS (Fig. 6, middle panel), as did, albeit less efficiently, moesin alone (Fig. 6, left panel), which has been implicated in the enhancement of MV uptake earlier. Most interestingly, however, substance P receptor, which assists in MV uptake into neural cells but also T cells by unknown mechanisms, also redistributes to the VS, where it tended to reveal a peripheral rather than a central localization (Fig. 6, right panel). Altogether, these analyses indicate that several MV receptors assisted by molecules strengthening adhesion might contribute to transmission at that particular structure.

DISCUSSION

The key role of CD150 expressing cells as early targets of MV infection and trafficking to secondary lymphatic tissues has been clearly revealed *in vitro* and *in vivo*, where they promote further dissemination by transmitting infectious MV to lymphocytes (2, 5, 8, 29). *In vitro* evidence suggests that the ability of MV to trigger DC maturation may be less efficient than that seen on lipopolysaccharide ligation and may even be compromised with regard to certain parameters such as chemokine receptor switching and CD40 signaling (reviewed in reference 39). MV-infected antigen-presenting cells surrounded by scanning lymphocytes have been documented in lymph nodes of experimentally macaques (29).

The role of DC-SIGN in capturing MV for enhancement of infection through CD150 has been clearly revealed *in vitro* (2, 7, 8), and yet the lack of DC-SIGN/CD150-coexpressing cells in subepithelial layers of the respiratory tract of healthy individuals has raised questions regarding the role of $DC\text{-}SIGN^+$ cells in early MV acquisition and led to the suggestion that these cells might preferentially trap virus for subsequent transmission. This particular study thus focused on *trans*-infection, where capture by DC-SIGN proved to be more important for both transmission and uptake for subsequent processing (8).

Our data clearly reveal that acquisition of MV by T cells is most efficient from *cis*-MV-DCs (Fig. 1A), which may well serve as transmission vectors also *in vivo*. This is because MV interaction with DC-SIGN caused activation of acid sphingomyelinase and subsequent vertical CD150 surface recruitment *in vitro* (2). In contrast to *trans*-infection (8), CD150-specific antibodies substantially interfered with *cis*-MV-DC transmission when added to

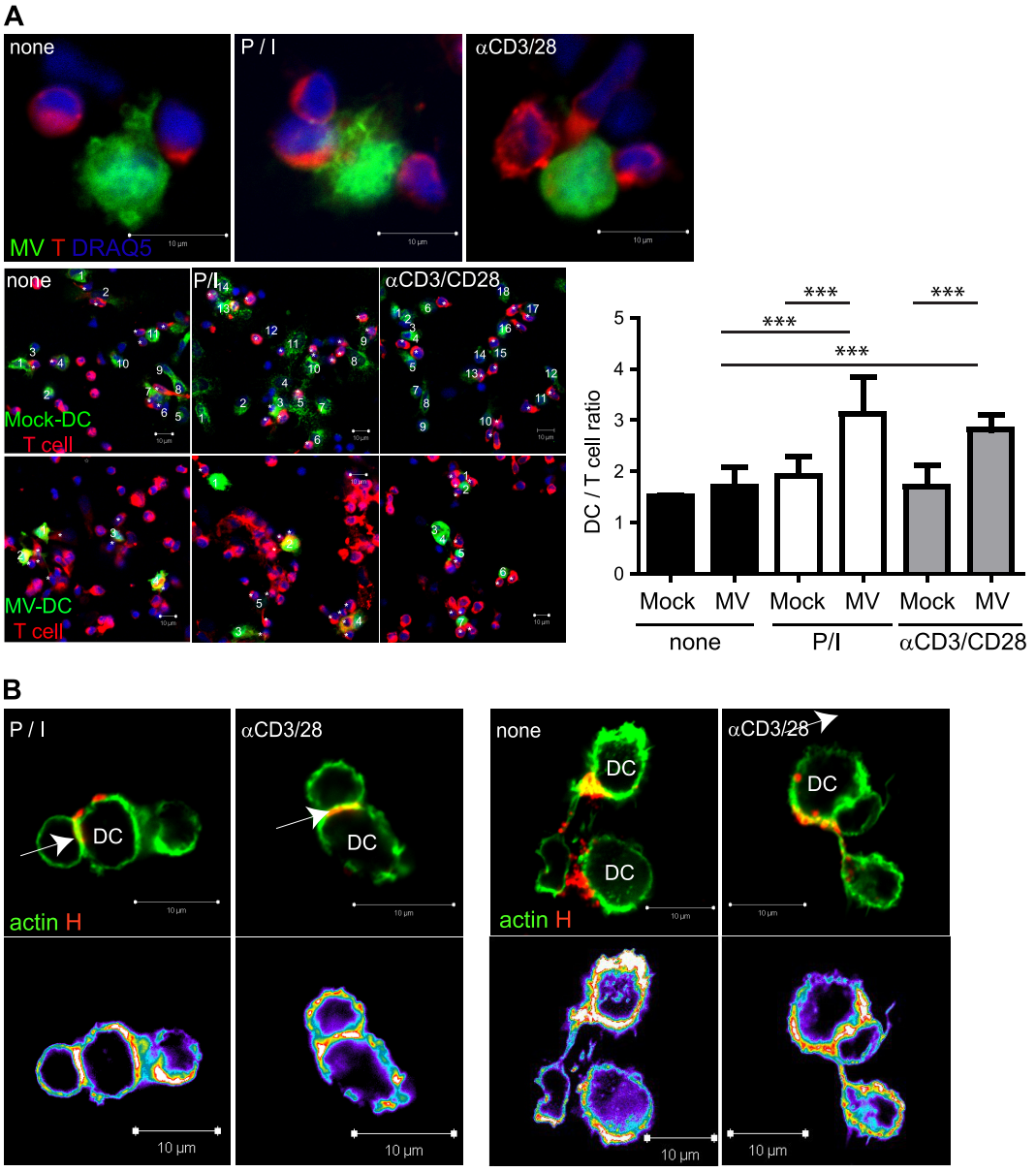

FIG 3 DC/T cell polyconjugates and filopodial bridges in MV-DC/T cell cocultures. (A) R18-labeled T cells (preactivated or not) were added to WGA-labeled Mock-DCs or IC323-eGFP-DCs seeded onto poly-L-lysine (PLL)-coated slides, and the frequencies of T cells conjugated per DC after 1 h were determined. Representative examples out of each 50 MV-DC conjugates are shown in the upper row, and examples for the enumeration of T cells (marked by asterisks) conjugated to WGA-labeled Mock-DCs (bottom panel, upper row) or MV-DCs (bottom panel, lower row) are marked by numbers, as are statistically relevant differences obtained upon the recruitment of 130 conjugates. ***, $P < 0.001$. (B) Conjugates involving MV WTF-DCs and T cells were stained with phalloidin-A488 and anti-MV H specific antibodies (K83). VS and filopodial bridges are indicated by arrows, and fluorescence intensity representations are shown at the bottom.

T cells but not DCs prior to coculture (Fig. 2B). Evidently, CD150 is efficiently redistributed to the contact interface in conjugated T cells (Fig. 4B and C), a finding which is line with the sensitivity of transmission efficiencies to blocking this receptor on the acceptor cell. CD150 expression on DCs is low and does not markedly increase after 24 h of infection (data not shown), indicating that the majority of endogenous CD150 detected at the MV VS is T cell derived (Fig. 4A). If the DC CD150 is also recruited there, it may not be of functional importance for transmission because homotypic interactions that might have a stabilizing effect may not occur given the higher avidity of the heterologous interaction with MV H protein (21), and prior exposure of DCs to CD150-specific antibodies does not impair subsequent transmission (data not shown).

Although in common with earlier observations for MV and also HIV (8, 11, 28, 45), we only infrequently observed MV in association with actin-enriched protrusions, most likely representing filopodial bridges (Fig. 3B). Though the formation of actin-based protrusions such as nanotubes *in vitro* may vary depending on the substrate (43), their relative importance in viral

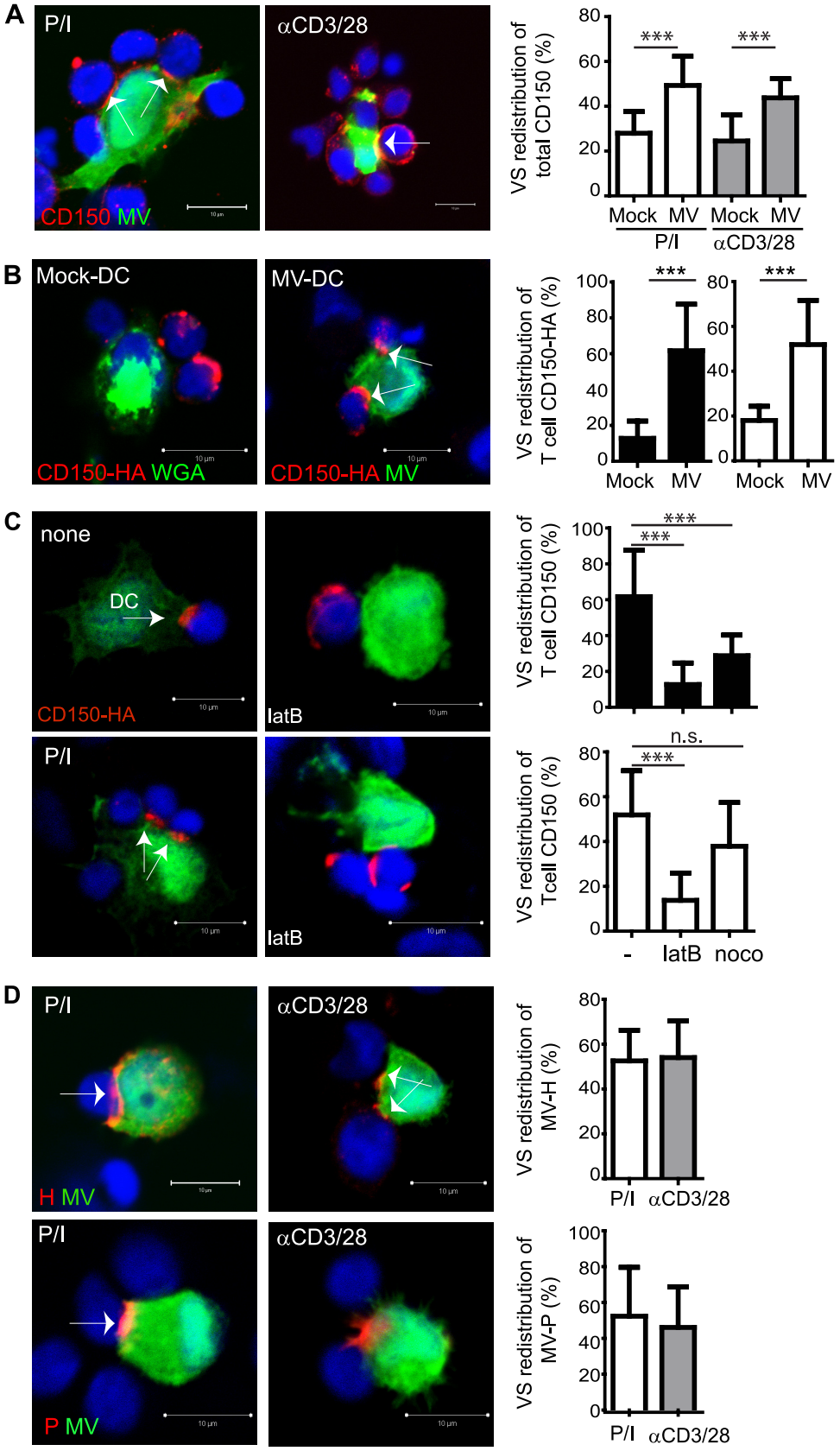

FIG 4 Viral proteins and MV entry receptor CD150 concentrate at the VS. Conjugates that formed between PLL-seeded IC323-eGFP-DCs (or WGA-labeled Mock-DCs) and T cells within 1 h were fixed and analyzed for VS redistribution of endogenous CD150 (A), CD150-HA transfected into T cells 24 h earlier (B and C), which, whether P/I preactivated or not, were pre-exposed to LatB or nocodazole (noco) for 1 h for MV H (C) or P (D) proteins. (A to D) VS are indicated by arrows (left), and quantifications of VS redistributions, shown on the right, involving at least 20 conjugates with T cells that were either unstimulated (■) or preactivated by P/I (□) or αCD3/CD28 (▨). Nuclei were counterstained using DRAQ5. ns, nonsignificant; ***, $P < 0.001$.

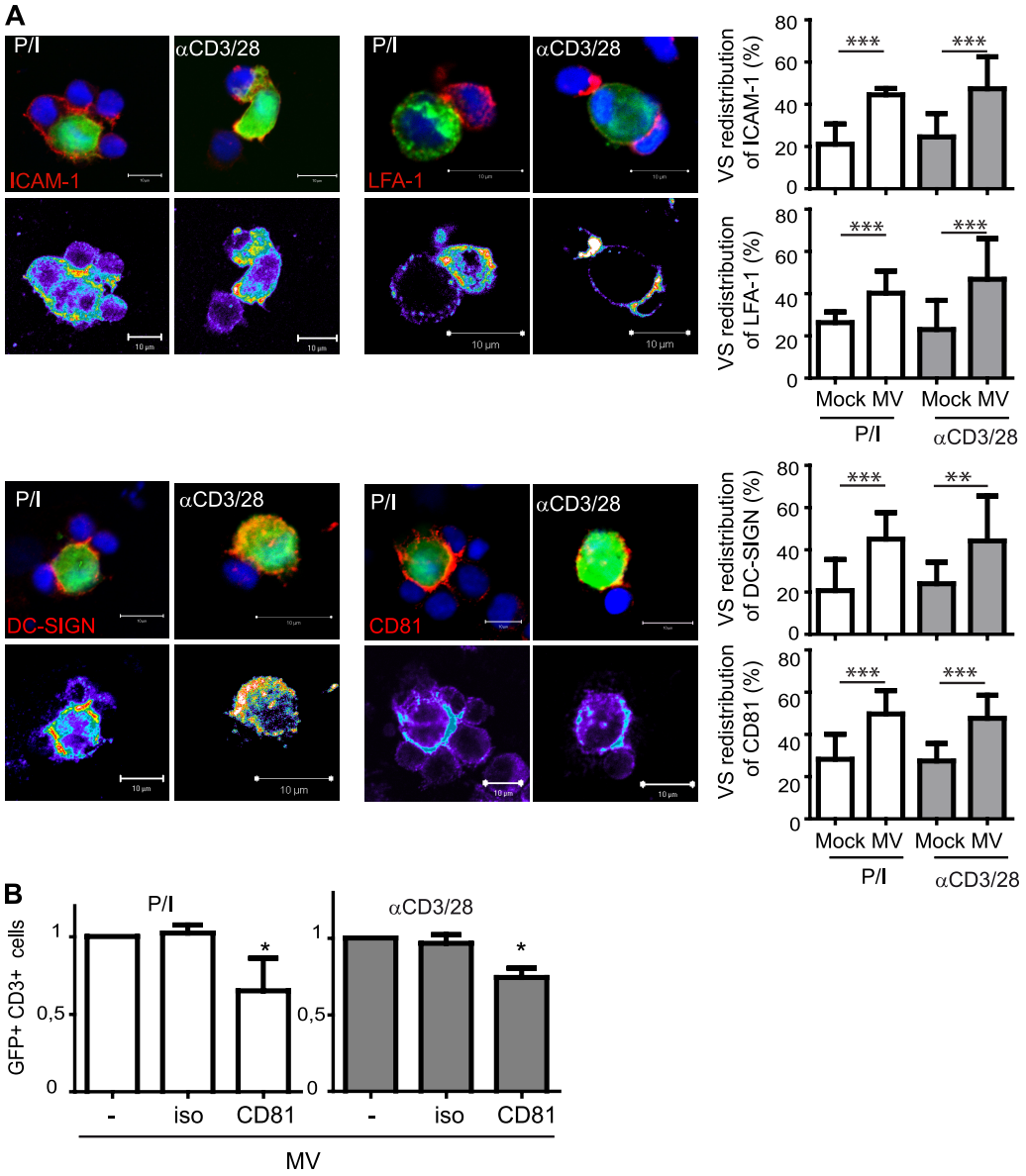

FIG 5 ICAM-1, LFA-1, DC-SIGN, and CD81 are VS components. (A) Conjugates formed between PLL-seeded IC323-eGFP-DCs and preactivated T cells within 1 h were fixed and analyzed for surface expression of ICAM-1 (upper left), activated LFA-1 (upper right), DC-SIGN (bottom left), or CD81 (bottom right). WGA-labeled Mock-DCs served as controls (right graphs). Values are expressed as the percentage of each total protein analyzed per layer. (B) MV-DCs were exposed to CD81 specific or isotype control antibodies at 1 h prior to coculture. Values obtained with untreated MV-DCs were set to 1. The means of three independent experiments (each performed in duplicates) are indicated by error bars representing standard deviations. *, $P < 0.05$; **, $P < 0.01$; ***, $P < 0.001$.

transmission *in vitro* has recently been questioned (34). The majority of transmission most likely occurs at contact interfaces between MV-DCs and T cells, which, given their similarity to those described for HIV, may be considered infectious synapses or VS (3, 18, 32). This is because both the major MV entry receptor and its ligand, H protein, and the P protein (used as RNP marker in our study) accumulate there, and cell-associated transmission from *cis*-infected DCs exceeds that by cell free virus 3-fold (Fig. 1, 3, and 4). An organized interface for MV transmission appears to be particularly important in view of the very limited ability of these cells to support the production of infectious particles (40). In common with the HIV VS (22, 23), viral proteins accumulate at the donor cell interface and while the major entry receptor, CD150, concentrates there in an actin-dependent manner (Fig. 4B and C). Whether VS accumulation of MV proteins in DCs was also actin dependent could not be analyzed because of the sensitivity of DC morphology and substrate adhesion on slides on prior exposure to nocodazole and LatB (data not shown), a finding is in line with earlier observations (49). As shown for T/T cell VS, Env interaction promoted recruitment of activated ERM proteins to the transmission site, and moesin was identified as a major component that is important in enhancing membrane fusion and HIV infection (3). We were also able to detect redistribution of pERM proteins and especially moesin toward the MV VS, and yet we did not resolve whether it occurs at the DC or T cell side (Fig. 6); moreover, it would have exceeded the scope of the present study to

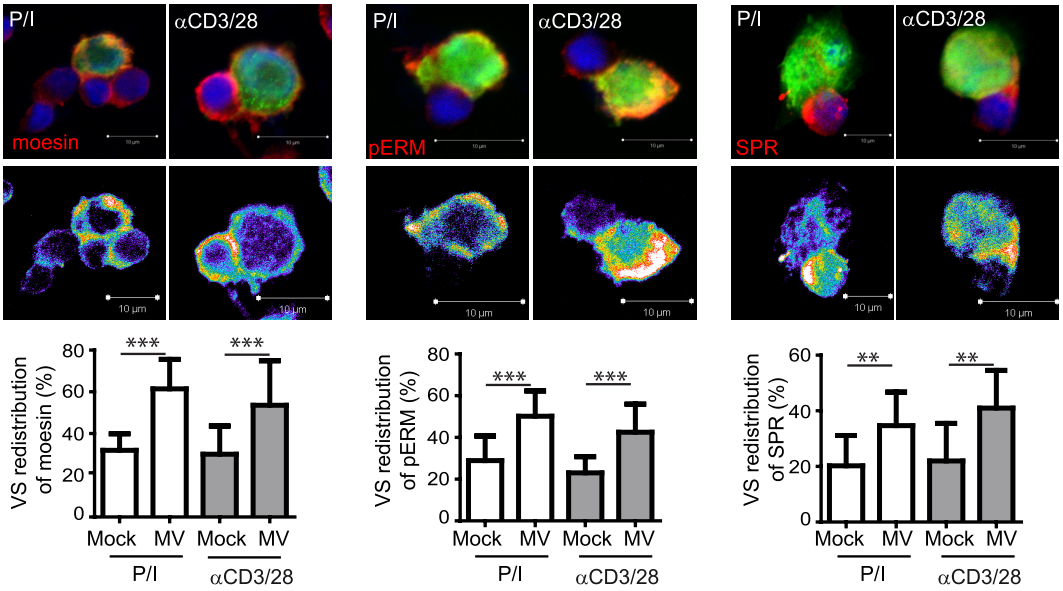

FIG 6 Phosphorylated ERM proteins and substance P receptor are VS components. Conjugates formed between PLL-seeded IC323-eGFP-DCs and preactivated T cells within 1 h were fixed and analyzed for the expression of moesin (upper left), pERM proteins (upper middle) or substance P receptor (SPR) (upper right). Intensity representations are shown in the bottom panels. WGA-labeled Mock-DCs served as controls (right graphs). **, $P < 0.01$; ***, $P < 0.001$.

resolve since this would causally relate to actin redistribution and/or local stabilization of actin-based protrusions, shown to be required for HIV entry (44) (Fig. 3B). Of note, however, is the fact that moesin has been found to assist in MV entry into target cells earlier, and its concentration at the VS is thus most likely of functional importance for transmission (9, 10). The loss of T-cell-receptor-stimulated ERM protein phosphorylation and actin-based protrusions on contact with MV glycoproteins with an unknown receptor, not identical to CD150, was found to occur in T cells (33), and thus the accumulation of pERM at the MV VS may imply that the inhibitory receptor is not compartmentalized there or that the inhibitory signal has extinguished by the time of conjugate analysis. When administered earlier, at conjugate formation, a signal-promoting pERM dephosphorylation concomitant with cofilin activation might even assist in the establishment of flattened contact planes by favoring actin remodeling. The latter may be fostered on VS redistribution of DC-SIGN (Fig. 5B) and subsequent signaling, as shown for HIV (12, 34). Whether DC-SIGN ligation in the MV VS promotes collapse of actin-based protrusions, as seen on MV-induced ceramide generation in T cells (14), or has a stabilizing function will be addressed in future experiments. ICAM-1 may further act to stabilize the structure via interaction with activated LFA-1 detected therein (Fig. 5A), as also suggested for the HIV VS (24). In common with other VS, CD3 did not polarize toward the MV-DC/T cell interface (data not shown) (25), and this will also apply to other molecules which are not recruited or, more interesting still, actively excluded from the MV-DC/T interface, the identification of which clearly exceeds the scope of present study.

Partitioning of CD81 to the HIV and MV VS has a role in viral transmission which, however, is only partially neutralized by specific antibodies (Fig. 5B), as already observed for CD150 (Fig. 2B), even upon the inclusion of higher antibody concentrations (data not shown). It is tempting to speculate that VS redistribution of several molecules previously shown to mediate or assist in MV entry creates a cooperative environment for efficient transmission. Notably, SPR apparently redistributes in T cells toward the VS, and, given its ability to support MV entry into T cells and cell-to-cell transmission in neurons, may play an active role in MV uptake (Fig. 6) (19, 20, 30). The similarity of the internal substance P FFG sequence with FIP and the N-terminal hydrophobic MV F1 fusion domain suggested it might, by interacting with the MV F protein, enhance fusion, which may well affect the sensitivity of this process to neutralizing antibodies (Fig. 2C). Thus, targeted ablation rather than antibody-based experiments will have to be conducted in order to evaluate the relative contributions of the MV VS components to stability and transmission mode and efficiency.

ACKNOWLEDGMENTS

We thank Jürgen Schneider-Schaulies, Paul Duprex, Bert Rima, Linda Rennick and Nora Müller for helpful discussions. We thank Y. Yanagi for providing IC-323-eGFP, Carl Figdor for providing the LFA-1 antibody, and Charlene Börtlein and Carolin Götz for excellent technical assistance.

We thank the Deutsche Forschungsgemeinschaft for financial support.

REFERENCES

1. **Albrecht P, Shabo AL, Burns GR, Tauraso NM.** 1972. Experimental measles encephalitis in normal and cyclophosphamide-treated rhesus monkeys. J. Infect. Dis. **126**:154–161.
2. **Avota E, Gulbins E, Schneider-Schaulies S.** 2011. DC-SIGN-mediated sphingomyelinase-activation and ceramide generation is essential for enhancement of viral uptake in dendritic cells. PLoS Pathog. **7**:e1001290. doi:10.1371/journal.ppat.1001290.
3. **Barrero-Villar M, et al.** 2009. Moesin is required for HIV-1-induced CD4-CXCR4 interaction, F-actin redistribution, membrane fusion, and viral infection in lymphocytes. J. Cell Sci. **122**:103–113.
4. **Condack C, Grivel JC, Devaux P, Margolis L, Cattaneo R.** 2007. Measles virus vaccine attenuation: suboptimal infection of lymphatic tissue and tropism alteration. J. Infect. Dis. **196**:541–549.
5. **de Swart RL, et al.** 2007. Predominant infection of CD150$^+$ lymphocytes

and dendritic cells during measles virus infection of macaques. PLoS Pathog. **3**:e178. doi:10.1371/journal.ppat.0030178.
6. **de Vries RD, et al.** 2010. *In vivo* tropism of attenuated and pathogenic measles virus expressing green fluorescent protein in macaques. J. Virol. **84**:4714–4724.
7. **de Witte L, Abt M, Schneider-Schaulies S, van Kooyk Y, Geijtenbeek TB.** 2006. Measles virus targets DC-SIGN to enhance dendritic cell infection. J. Virol. **80**:3477–3486.
8. **de Witte L, et al.** 2008. DC-SIGN and CD150 have distinct roles in transmission of measles virus from dendritic cells to T-lymphocytes. PLoS Pathog. **4**:e1000049. doi:10.1371/journal.ppat.1000049.
9. **Dunster LM, et al.** 1995. Moesin, and not the murine functional homologue (Crry/p65) of human membrane cofactor protein (CD46), is involved in the entry of measles virus (strain Edmonston) into susceptible murine cell lines. J. Gen. Virol. **76**(Pt 8):2085–2089.
10. **Dunster LM, et al.** 1994. Moesin: a cell membrane protein linked with susceptibility to measles virus infection. Virology **198**:265–274.
11. **Eugenin EA, Gaskill PJ, Berman JW.** 2009. Tunneling nanotubes (TNT) are induced by HIV-infection of macrophages: a potential mechanism for intercellular HIV trafficking. Cell. Immunol. **254**:142–148.
12. **Felts RL, et al.** 2010. 3D visualization of HIV transfer at the virological synapse between dendritic cells and T cells. Proc. Natl. Acad. Sci. U. S. A. **107**:13336–13341.
13. **Ferreira CS, et al.** 2010. Measles virus infection of alveolar macrophages and dendritic cells precedes spread to lymphatic organs in transgenic mice expressing human signaling lymphocytic activation molecule (SLAM, CD150). J. Virol. **84**:3033–3042.
14. **Gassert E, et al.** 2009. Induction of membrane ceramides: a novel strategy to interfere with T lymphocyte cytoskeletal reorganisation in viral immunosuppression. PLoS Pathog. **5**:e1000623. doi:10.1371/journal.ppat.1000623.
15. **Griffin DE.** 2010. Measles virus-induced suppression of immune responses. Immunol. Rev. **236**:176–189.
16. **Grosjean I, et al.** 1997. Measles virus infects human dendritic cells and blocks their allostimulatory properties for $CD4^+$ T cells. J. Exp. Med. **186**:801–812.
17. **Hahm B, Arbour N, Oldstone MB.** 2004. Measles virus interacts with human SLAM receptor on dendritic cells to cause immunosuppression. Virology **323**:292–302.
18. **Haller C, Fackler OT.** 2008. HIV-1 at the immunological and T-lymphocytic virological synapse. Biol. Chem. **389**:1253–1260.
19. **Harrowe G, Mitsuhashi M, Payan DG.** 1990. Measles virus-substance P receptor interactions: possible novel mechanism of viral fusion. J. Clin. Invest. **85**:1324–1327.
20. **Harrowe G, Sudduth-Klinger J, Payan DG.** 1992. Measles virus-substance P receptor interaction: Jurkat lymphocytes transfected with substance P receptor cDNA enhance measles virus fusion and replication. Cell. Mol. Neurobiol. **12**:397–409.
21. **Hashiguchi T, et al.** 2011. Structure of the measles virus hemagglutinin bound to its cellular receptor SLAM. Nat. Struct. Mol. Biol. **18**:135–141.
22. **Iyengar S, Hildreth JE, Schwartz DH.** 1998. Actin-dependent receptor colocalization required for human immunodeficiency virus entry into host cells. J. Virol. **72**:5251–5255.
23. **Jimenez-Baranda S, et al.** 2007. Filamin-A regulates actin-dependent clustering of HIV receptors. Nat. Cell Biol. **9**:838–846.
24. **Jolly C, Mitar I, Sattentau QJ.** 2007. Adhesion molecule interactions facilitate human immunodeficiency virus type 1-induced virological synapse formation between T cells. J. Virol. **81**:13916–13921.
25. **Jolly C, Sattentau QJ.** 2004. Retroviral spread by induction of virological synapses. Traffic **5**:643–650.
26. **Kerdiles YM, Sellin CI, Druelle J, Horvat B.** 2006. Immunosuppression caused by measles virus: role of viral proteins. Rev. Med. Virol. **16**:49–63.
27. **Kobune F, et al.** 1996. Nonhuman primate models of measles. Lab. Anim. Sci. **46**:315–320.
28. **Lehmann M, Nikolic DS, Piguet V.** 2011. How HIV-1 takes advantage of the cytoskeleton during replication and cell-to-cell transmission. Viruses **3**:1757–1776.
29. **Lemon K, et al.** 2011. Early target cells of measles virus after aerosol infection of non-human primates. PLoS Pathog. **7**:e1001263. doi:10.1371/journal.ppat.1001263.
30. **Makhortova NR, et al.** 2007. Neurokinin-1 enables measles virus trans-synaptic spread in neurons. Virology **362**:235–244.
31. **McChesney MB, Fujinami RS, Lerche NW, Marx PA, Oldstone MB.** 1989. Virus-induced immunosuppression: infection of peripheral blood mononuclear cells and suppression of immunoglobulin synthesis during natural measles virus infection of rhesus monkeys. J. Infect. Dis. **159**:757–760.
32. **McDonald D, et al.** 2003. Recruitment of HIV and its receptors to dendritic cell-T cell junctions. Science **300**:1295–1297.
33. **Muller N, et al.** 2006. Measles virus contact with T cells impedes cytoskeletal remodeling associated with spreading, polarization, and CD3 clustering. Traffic **7**:849–858.
34. **Nikolic DS, et al.** 2011. HIV-1 activates Cdc42 and induces membrane extensions in immature dendritic cells to facilitate cell-to-cell virus propagation. Blood **118**:4841–4852.
35. **Ohno S, et al.** 2007. Measles virus infection of SLAM (CD150) knockin mice reproduces tropism and immunosuppression in human infection. J. Virol. **81**:1650–1659.
36. **Okada H, et al.** 2000. Extensive lymphopenia due to apoptosis of uninfected lymphocytes in acute measles patients. Arch. Virol. **145**:905–920.
37. **Pohl C, Shishkova J, Schneider-Schaulies S.** 2007. Viruses and dendritic cells: enemy mine. Cell Microbiol. **9**:279–289.
38. **Schneider-Schaulies J, Dunster LM, Schwartz-Albiez R, Krohne G, ter Meulen V.** 1995. Physical association of moesin and CD46 as a receptor complex for measles virus. J. Virol. **69**:2248–2256.
39. **Schneider-Schaulies S, Schneider-Schaulies J.** 2009. Measles virus-induced immunosuppression. Curr. Top. Microbiol. Immunol. **330**:243–269.
40. **Servet-Delprat C, et al.** 2000. Measles virus induces abnormal differentiation of CD40 ligand-activated human dendritic cells. J. Immunol. **164**:1753–1760.
41. **Servet-Delprat C, Vidalain PO, Valentin H, Rabourdin-Combe C.** 2003. Measles virus and dendritic cell functions: how specific response cohabits with immunosuppression. Curr. Top. Microbiol. Immunol. **276**:103–123.
42. **Shishkova Y, Harms H, Krohne G, Avota E, Schneider-Schaulies S.** 2007. Immune synapses formed with measles virus-infected dendritic cells are unstable and fail to sustain T cell activation. Cell Microbiol. **9**:1974–1986.
43. **Sowinski S, Alakoskela JM, Jolly C, Davis DM.** 2011. Optimized methods for imaging membrane nanotubes between T cells and trafficking of HIV-1. Methods **53**:27–33.
44. **Steffens CM, Hope TJ.** 2003. Localization of CD4 and CCR5 in living cells. J. Virol. **77**:4985–4991.
45. **Stolp B, Fackler OT.** 2011. How HIV takes advantage of the cytoskeleton in entry and replication. Viruses **3**:293–311.
46. **Tran-Van H, Avota E, Bortlein C, Mueller N, Schneider-Schaulies S.** 2011. Measles virus modulates dendritic cell/T-cell communication at the level of plexinA1/neuropilin-1 recruitment and activity. Eur. J. Immunol. **41**:151–163.
47. **van Binnendijk RS, Poelen MC, van Amerongen G, de Vries P, Osterhaus AD.** 1997. Protective immunity in macaques vaccinated with live attenuated, recombinant, and subunit measles vaccines in the presence of passively acquired antibodies. J. Infect. Dis. **175**:524–532.
48. **van der Vlist M, et al.** 2011. Human Langerhans cells capture measles virus through Langerin and present viral antigens to CD4 T cells but are incapable of cross-presentation. Eur. J. Immunol. **41**:2619–2631.
49. **Wang JH, Wells C, Wu L.** 2008. Macropinocytosis and cytoskeleton contribute to dendritic cell-mediated HIV-1 transmission to $CD4^+$ T cells. Virology **381**:143–154.
50. **Yanagi Y, Takeda M, Ohno S.** 2006. Measles virus: cellular receptors, tropism and pathogenesis. J. Gen. Virol. **87**:2767–2779.